Multistage nonlinear optimization to recover neural activation patterns from evoked compound action potentials of cochlear implant users

Stefano Cosentino, Etienne Gaudrain, John Deeks, Robert P. Carlyon

This article has been accepted for publication in a future issue of this journal, but has not been fully edited. Content may change prior to final publication. Citation information: DOI 10.1109/TBME.2015.2476373, IEEE Transactions on Biomedical Engineering

Multistage nonlinear optimization to recover neural activation patterns from evoked compound action potentials of cochlear implant users

Stefano Cosentino, Etienne Gaudrain, John M. Deeks, and Robert P. Carlyon

***Abstract*— *Objective:* Electrically evoked compound action potentials (ECAPs) have been employed as a measure of neural activation evoked by cochlear implant (CI) stimulation. A forward-masking procedure is commonly used to reduce stimulus artefacts. This method estimates the joint neural activation produced by two electrodes – one acting as probe and the other as masker; as such, the measured ECAPs depend on the activation patterns produced by both. We describe an approach - termed Panoramic ECAP ("PECAP") - that allows reconstruction of the underlying neural activation pattern of individual channels from ECAP amplitudes. *Methods:* The proposed approach combines two constrained nonlinear optimization stages. PECAP was validated against simulated and physiological data from CI users. The physiological data consisted of ECAPs measured from four users of Cochlear® devices. For each subject, an 18×18 ECAP amplitude matrix was measured using a forward-masking method. *Results:* The results from computer simulations indicate that our approach can reliably estimate the underlying activation patterns from ECAP amplitudes even for instances of neural "dead regions" or cross-turn stimulation. The operating signal-to-noise ratio (SNR) for the proposed algorithm was 5 dB or higher, which matched well the SNR measured from human physiological data. Human ECAPs were fitted with our procedure to determine neural activation patterns. *Conclusion:* PECAP can be used to identify undesirable features of the neural activation pattern of individual CI users. *Significance:* Our approach may have clinical application as an objective measure of electrode-to-neuron interface and may be used to devise *ad hoc* stimulation strategies.**

***Index Terms*— neural activation patterns, cochlear implant, ECAP, optimization.**

Submitted for review on June 23, 2015. This work was supported by the Medical Research Council UK (MC-A060-5PQ70) and by Action on Hearing Loss (MC-A060-5PQ75).

Authors were with MRC - Cognition and Brain Sciences Unit, Cambridge, CB2 7EF (UK) at the time of the research (correspondence e-mail: stefano.cosentino@mrc-cbu.cam.ac.uk).

Author E.G. is with Centre de Recherche en Neurosciences de Lyon - CNRS UMR 5292, Université Lyon 1, 69366 Lyon Cedex 7 (France).

I. Introduction

THE electrically evoked compound action potential (ECAP) is thought to reflect the compound activity of auditory nerve fibres that are electrically stimulated. ECAPs are often used as clinical objective diagnostics for cochlear implant (CI) users both during and after implantation. They provide a fast non-invasive measure of the compound auditory nerve response, without the need for any behavioural response from the patient. Yet, the scarce correlation between ECAPs and behavioural measurements within and across subjects has led some of the research community to question the usefulness of ECAPs [1-3]. One aim of the present study is to propose a method of processing ECAP amplitude data that provides a more valid measure of neural activation patterns.

One concern about the reliability of the measured ECAP relates to the size of the measured evoked response, which is generally several orders of magnitude smaller than that of the stimulus used to evoke that response. As such, it is essential to employ a recording paradigm capable of attenuating the stimulation artifact. The most common and reliable (see Cohen, et al. [4]) approach to achieve this is by using a forward-masking paradigm first described by Brown, et al. [5]. This paradigm involves obtaining four responses to, respectively, a) a probe pulse, b) probe preceded by a masker pulse, c) masker alone, d) non-stimulation. By adding and subtracting the responses according to the formula $ECAP = a - (b - c) - d$ one can obtain the neural response to the probe uncontaminated by stimulus artifact or DC bias (see Fig. 1 for a schematic of the method).

In a clinical context, forward-masking ECAPs have often been used to measure neural response for a given current level, in conditions where both masker and probe are on the same electrode. Researchers have expanded this approach to measure the ECAP amplitude for each electrode combination ("ECAP masking pattern"), in a paradigm where either the probe position is fixed and masker position is varied [4], or *vice versa* [6].

The forward-masking ECAP for any combination of masker and probe electrode will reflect two main contributions. First, it will depend on the total neural activation produced by the stimulation of the probe electrode. Second, the measured

This article has been accepted for publication in a future issue of this journal, but has not been fully edited. Content may change prior to final publication. Citation information: DOI 10.1109/TBME.2015.2476373, IEEE Transactions on Biomedical Engineering

ECAP will depend on the proportion of the probe response that is not masked by the masker, which we can term k. If masking is complete, $k = 0$ and the measured ECAP will mostly reflect the neural activation due to the probe. Hence, for each masker/probe electrode combination, the measured ECAP will reflect the proportion of the neural response to the probe that is masked by the masker, i.e. their joint activation pattern, which can be expressed as:

$$ECAP \sim (1 - k) \cdot p \quad (1)$$

where p is the neural activation produced by the probe.

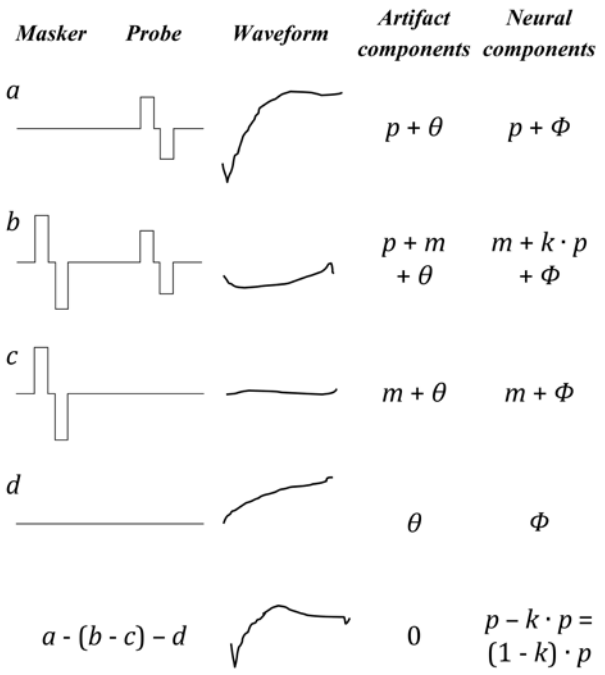

Fig. 1. Schematics of forward-masking paradigm. Last two columns report the artifact and neural components that are produced after each waveform by the following sources: $\boldsymbol{p}$ ~ probe, $\boldsymbol{m}$ ~ masker, $\boldsymbol{\Phi}$ ~ baseline activity, $\boldsymbol{\theta}$ ~ amplifier switch-on; $\boldsymbol{k}$ is the proportion of the probe neural response that is not masked by the masker.

Crucially, this measure relies on the masker reducing the neural response to the probe and hence reflects the amount of neural overlap between the neural "activation patterns" (AP, also known as "excitation pattern") elicited by the masker and probe. Hence when interpreting the size of any single ECAP it is not possible to determine the AP of either the masker or probe electrode.

Previous research has treated ECAP masking patterns as direct measures of neural activation patterns, but the reasoning of the current study is not in agreement with this view, as can be illustrated by a simple extreme example. Consider the case where the neural APs for a number of electrodes are Gaussian with widths of the patterns for odd electrodes being four times as broad as for even electrodes (shown in Fig. 2b). The simulation in Fig. 2a shows the predicted ECAP masking pattern that would be measured with masker on electrode 9 ("E9"), derived by multiplying the excitation pattern for E9 with that for each of the other electrodes. It shows a "zig-zag" effect, being large near odd-numbered electrodes and small near even-numbered electrodes. This effect is due to the excitation patterns of the other electrodes rather than to E9, and so is misleading.

Our approach, termed Panoramic ECAP (PECAP), is to disambiguate this information by recording ECAPs to every possible combination of masker and probe. In order to achieve a mathematically tractable solution, we make assumptions on both the production of the ECAP (the ECAP amplitude model described in II.A) and on the properties of the neural activation patterns (described in II.C). If these assumptions hold, the proposed method can recover the AP from the ECAP amplitudes.

A second objective for the proposed method is to be able to detect "unwanted exceptions" in the electrode-to-neuron mapping. Such exceptions are instances of poor spatial selectivity that are likely to reduce the benefit that patients obtain from their CI. One such case is referred to as neural dead regions; if neurons near a given electrode have not survived, then stimulating that electrode will produce maximal excitation at one or more additional places, typically near adjacent electrodes. Another unwanted exception is caused by cross-turn stimulation. In this case, stimulating an electrode at, e.g., the apex, can cause current to spread to another cochlear turn. Cross-turn stimulation often results in an additional peak in the neural excitation pattern at a point several electrodes away from the one that is stimulated. Finally, ectopic stimulation can sometimes occur, where the return current exits near the base of cochlea, even when current is injected to an apical electrode, thereby exciting basal auditory nerve fibers [7]. As a first step, we describe a method that is capable of detecting instances of "unwanted exceptions" on a single electrode per subject.

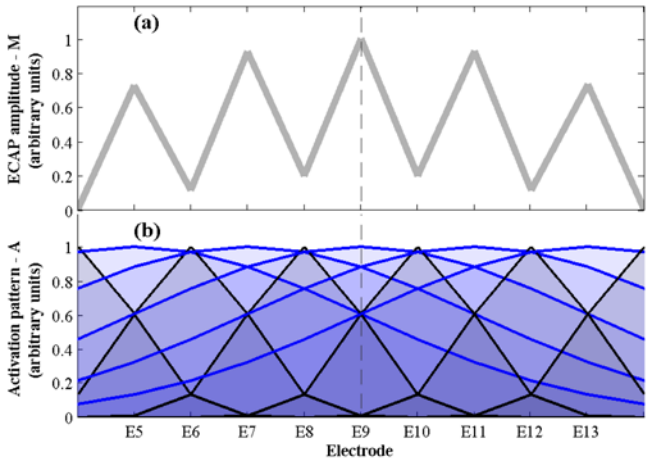

Fig. 2. Illustrative example of (**a**) simulated ECAP masking pattern measured on E9 and (**b**) excitation patterns for E5 to E13.

II. Methods

A. ECAP amplitude Model

The proposed approach to recover AP from ECAP

This article has been accepted for publication in a future issue of this journal, but has not been fully edited. Content may change prior to final publication. Citation information: DOI 10.1109/TBME.2015.2476373, IEEE Transactions on Biomedical Engineering

amplitudes, termed PECAP, relies on a simple model of forward-masking ECAPs. The necessary assumptions are reported below along with a description of the model. A discussion of these assumptions can be found in section IV.

i. Symmetry assumption

The model assumes that ECAPs are generated by the joint neural activation pattern of both probe and masker electrodes, thus the ECAP amplitude for a given combination of probe and masker electrodes (p, m) can be expressed as:

$$M_{p,m} = \sum_k A_p(k) \cdot A_m(k) \tag{2}$$

where $A_i(k)$ is the neural AP produced by electrode i stimulated at most comfortable level (MCL) as function of place k along the cochlea. Let us define a set of electrodes N : $(p, m) \in N$. The matrix containing the ECAP amplitudes for all combinations of p and m will be:

$$\boldsymbol{M} = \boldsymbol{A} \cdot \boldsymbol{A}^T \tag{3}$$

Hereafter, $\boldsymbol{M}$ is the matrix containing the ECAP amplitudes obtained with forward-masking method and is assumed to be symmetric.

ii. The AP can be modelled with Gaussian functions

The neural activation A_i for electrode i is modelled as a Gaussian, i.e. each row of $\boldsymbol{A}$ is a Gaussian controlled by three parameters: mean (μ), standard deviation (σ) and amplitude (α), so that:

$$A_i(k) = \alpha_i \cdot e^{-\frac{(k-\mu_i)^2}{2\cdot\sigma_i}} \tag{4}$$

Let us denote with $\boldsymbol{B}$ the parameter vector containing μ, σ and α for each row of $\boldsymbol{A}$.

iii. The APs at fixed MCL have equal area

If electrodes are stimulated at the same loudness level (e.g., at MCL), we assume that the area under the excitation patterns for different electrodes is roughly the same. Hence, the amplitude parameter α is a dependent variable of both mean (μ) and width (σ), and $\boldsymbol{B}$ can be simplified as:

$$\boldsymbol{B} = \begin{bmatrix} \mu_1 & \sigma_1 \\ \vdots & \vdots \\ \mu_N & \sigma_N \end{bmatrix} \tag{5}$$

B. The inverse problem

Given a set of ECAP amplitude measurements $\widehat{\boldsymbol{M}}$ and measurement noise $\boldsymbol{\varepsilon}$,

$$\widehat{\boldsymbol{M}} = \boldsymbol{M} + \boldsymbol{\varepsilon}, \tag{6}$$

we are interested in recovering the parameters in $\boldsymbol{B}$ of the Gaussians that approximate the true neural activation patterns $\boldsymbol{A}$ as:

$$\widehat{\boldsymbol{B}} = \begin{bmatrix} \hat{\mu}_1 & \hat{\sigma}_1 \\ \vdots & \vdots \\ \hat{\mu}_N & \hat{\sigma}_N \end{bmatrix} \rightarrow \begin{cases} \boldsymbol{A} = \boldsymbol{A}_{\widehat{\boldsymbol{B}}} \\ \boldsymbol{M} = \boldsymbol{A}_{\widehat{\boldsymbol{B}}} \cdot \boldsymbol{A}_{\widehat{\boldsymbol{B}}}{}^T \end{cases} \tag{7}$$

where $\boldsymbol{A}_{\widehat{\boldsymbol{B}}}$ is the AP reconstructed using Eq. 4 with means and widths contained in $\widehat{\boldsymbol{B}}$. Since the solution is not unique, a numerical approach is followed instead, as described next.

C. PECAP approach

1) Optimization overview

PECAP consists of a multi-stage nonlinear optimization. The combination of constrained (STAGE I) and less-constrained (STAGE II) optimizations is necessary because the system is undetermined, thus the solution is generally not unique: for a given ECAP amplitude measurement matrix $\boldsymbol{M}$ there is not a unique neural activation pattern $\boldsymbol{A}$ that can produce it. A first optimization stage is run where strong assumptions are made on the activation patterns to be recovered. A second stage follows where potential exceptions to the simple ECAP model described above are to be detected.

2) STAGE I: constrained nonlinear optimization

Stage I of the PECAP approach includes the following main steps. First, the average along the diagonal of $\widehat{\boldsymbol{M}}$ is computed:

$$\boldsymbol{M_s} = \frac{\widehat{\boldsymbol{M}} + \widehat{\boldsymbol{M}}^{\boldsymbol{T}}}{\boldsymbol{2}} \tag{8}$$

This is possible having assumed symmetry in the ECAP amplitude model, $M_{p,m} = M_{m,p}$. By computing $\boldsymbol{M_s}$ the measurement noise $\boldsymbol{\varepsilon}$ should be reduced, under the general assumption that $\boldsymbol{\varepsilon}$ is normally distributed [8].

Second, the parameters of $\boldsymbol{B}$ are found that minimize the error:

$$\boldsymbol{\epsilon_M} = \left|\boldsymbol{M}_{\widehat{\boldsymbol{B}}} - \boldsymbol{M_s}\right| = \left|\boldsymbol{A}_{\widehat{\boldsymbol{B}}} \cdot \boldsymbol{A}_{\widehat{\boldsymbol{B}}}{}^T - \boldsymbol{M_s}\right| \tag{9}$$

A constrained nonlinear optimization algorithm based on the Barrier method [9] is employed to find the minimum for Eq. 9. For any electrode p, the following constraints are imposed:

$$\begin{matrix} a) \\ b) \\ c) \end{matrix} \quad \begin{cases} \left|\mu_p - p\right| < 0.5 \\ \mu_{p-1} \leq \mu_p \leq \mu_{p+1} \\ 0 < \sigma_p \leq 6 \end{cases} \tag{10}$$

The first two constraints ensure the modelled means of the excitation patterns are within 0.5 electrode spacing from the expected mean (note that *b*) is always true when *a*) is). Constraint *c*) imposes an upper limit on the widths of the Gaussians.

3) STAGE II: partially constrained optimization to detect exceptions

The approach in STAGE I to minimize the error in Eq. 9 is

This article has been accepted for publication in a future issue of this journal, but has not been fully edited. Content may change prior to final publication. Citation information: DOI 10.1109/TBME.2015.2476373, IEEE Transactions on Biomedical Engineering

highly constrained, and while it prevents solutions with *unrealistic* electrode-to-neuron mappings, *realistic* exceptions in the activation patterns such as dead regions or cross-turn stimulations might be undetected. Hence, a second optimization step is run where constraints are relaxed in a row-by-row order in $\boldsymbol{A}$ to allow instances of dead regions or cross-turn stimulations to be detected. This is obtained through two parallel steps run in parallel:

1) STAGE II (SP): For each probe electrode p, the error in Eq. 9 is computed relaxing constraints *a*) and *b*) in Eq. 10 ($\boldsymbol{A}_i$ for $i \neq p$ will still be constrained) yielding an updated parameter vector $\widehat{\boldsymbol{B}}'$. A dead region is detected if the new fit produces a smaller error such that:

$$\boldsymbol{\epsilon_M} - \left|\boldsymbol{A}_{\widehat{\boldsymbol{B}}'} \cdot \boldsymbol{A}_{\widehat{\boldsymbol{B}}'}{}^{T} - \boldsymbol{M_S}\right| \geq \beta \boldsymbol{\epsilon_M} \qquad (11)$$

$\beta = 10\%$ was derived empirically as a threshold for the reduction in error to be significant.

2) STAGE II (BI): A stage similar to that described above is in use to detect instances of cross-turn stimulation. Specifically, for each p the error in Eq. 9 is computed relaxing the constraints in Eq. 10 and allowing A_p to be bimodal. Hence, the updated parameter vector $\widehat{\boldsymbol{B}}'$ contains two additional values: the mean and the standard deviation of the second peak in the bimodal A_p. An instance of cross-turn stimulation is detected if the new fit produces a smaller error as per Eq. 11. Whenever both the first and second steps of STAGE II fulfil Eq. 11 for a given probe electrode, the larger of the two improvements will be taken as indication of either a shifted peak or of bimodality.

The search for exceptions in the neural activation carried out in STAGE II is restricted to instances of *single* exceptions: if one or more electrodes are in a dead region or produce cross-turn stimulation, STAGE II will likely fail to detect them. This limitation is discussed further in section IV.

III. Data Validation

Three tests were designed to validate the PECAP approach and, indirectly, the ECAP amplitude model also described in section II. Both simulated and actual CI data were used.

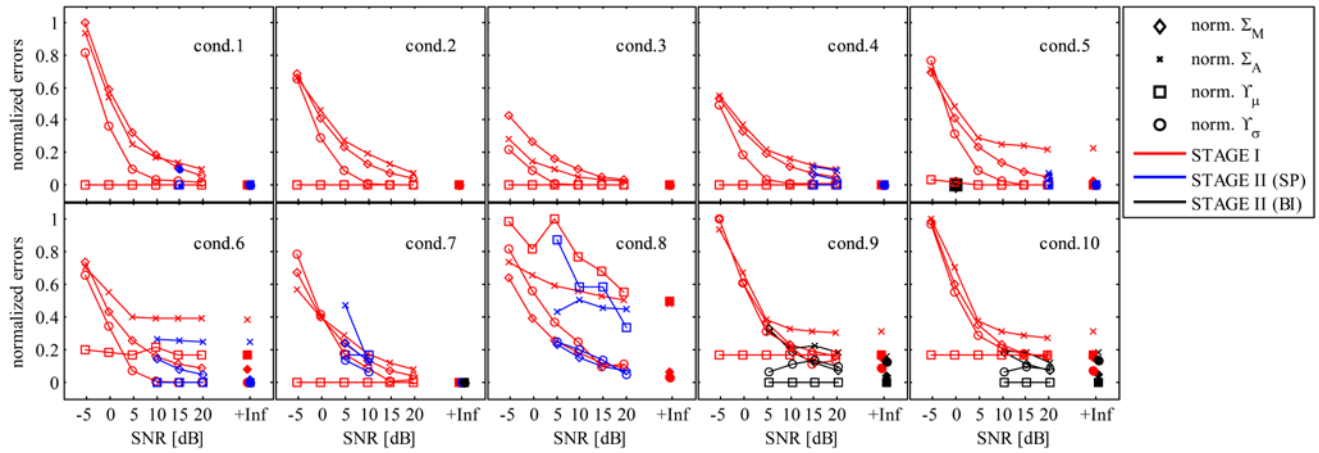

Fig. 1. Error metrics as function of SNR estimated for the computer simulation results of Test 1. To aid readability, each metric was normalized across the ten conditions. Note that normalized errors should not be compared *across* metrics. Color image online.

A. Test 1: Simulated data

1) Stimuli and methods

Simulated measurement $\boldsymbol{M}$s were generated using the model described in II.A. In order to validate the ability of PECAP to predict activation patterns $\boldsymbol{A}$ known *a priori*, $\boldsymbol{M}$s were generated for a number of different conditions and at different signal-to-noise ratios (SNRs). Different SNRs were obtained by adjusting the RMS of a noise matrix ($\boldsymbol{\varepsilon}$ in Eq. 6) which was linearly added to the simulated $\boldsymbol{M}$. The parameters were chosen to simulate ten conditions that encompass possible neural activation scenarios and that are reported in Table 1. Conditions 1-3 simulate scenarios where the neural activation are centred on the stimulating electrode (i.e., the *expected* mean values), whereas their widths can be between 0.5 and 5 for all electrodes. In condition 4 the widths of odd electrodes differ significantly from the widths of the even electrodes (this example was also described in section I). Condition 5 simulates a dead region, where the neural activation for E8 peaks on E9. In Condition 6, both E8 and E9 are displaced and their APs peak on E10. Condition 7 simulates variable widths (in the range of 0.2 and 3.5) across different electrodes. Condition 8 combines the variable widths of condition 7 with variable means, thus reflecting a very heterogeneous neural survival in the cochlea. Finally, conditions 9 and 10 simulate instances of bimodality where E8 has a second peak in the activation pattern that is 6 or 10 electrodes basally to the probe, respectively.

2) Simulation results and discussion

Four metrics were used to quantify the discrepancy between true values and those produced by the PECAP reconstruction.

This article has been accepted for publication in a future issue of this journal, but has not been fully edited. Content may change prior to final publication. Citation information: DOI 10.1109/TBME.2015.2476373, IEEE Transactions on Biomedical Engineering

Two metrics are the RMSE computed between true and fitted neural activation patterns $\boldsymbol{A}$ (Σ_A), and between true and reconstructed measurement matrix $\boldsymbol{M}$ (Σ_M). Two more metrics are the number of cases where the mean or width in the modelled APs differ from true values by more than a fixed

TABLE 1. PARAMETERS CHOSEN FOR THE 10 CONDITIONS (COLUMNS (i) AND (ii)) AND RESULTS OF THE COMPUTER SIMULATION (COLUMNS (iii) AND (iv)).

Simulated condition		*Channels* 3	4	5	6	7	8	9	10	11	12	13	14	15	16	17	18	19	20	E_{bim}	*Absolute error after STAGE I.* Σ_A	Σ_M	Υ_μ	Υ_σ	*Percent improvement after STAGE II.* Σ_A	Σ_M	Υ_μ	Υ_σ
1. Canonical with narrow widths	μ	3	4	5	6	7	8	9	10	11	12	13	14	15	16	17	18	19	20	-	1.14	0.14	0.00	2.90	↑84	↑86	0.0	↑100
	σ	.5	.5	.5	.5	.5	.5	.5	.5	.5	.5	.5	.5	.5	.5	.5	.5	.5	.5	-								
2. Canonical with unit widths	μ	3	4	5	6	7	8	9	10	11	12	13	14	15	16	17	18	19	20	-	0.79	0.12	0.00	2.30	-	-	-	-
	σ	1	1	1	1	1	1	1	1	1	1	1	1	1	1	1	1	1	1	-								
3. Canonical with wide widths	μ	3	4	5	6	7	8	9	10	11	12	13	14	15	16	17	18	19	20	-	0.52	0.04	0.00	0.70	-	-	-	-
	σ	5	5	5	5	5	5	5	5	5	5	5	5	5	5	5	5	5	5	-								
4. Zig-zag widths	μ	3	4	5	6	7	8	9	10	11	12	13	14	15	16	17	18	19	20	-	0.65	0.10	0.00	1.60	↑83	↑70	0.0	↑100
	σ	4	1	4	1	4	1	4	1	4	1	4	1	4	1	4	1	4	1	-								
5. Displaced E8	μ	3	4	5	6	7	9	9	10	11	12	13	14	15	16	17	18	19	20	-	0.82	0.16	0.04	2.60	↑90	↑88	↑100	↑100
	σ	1	1	1	1	1	1	1	1	1	1	1	1	1	1	1	1	1	1	-								
6. Displaced E8, E9 on E10	μ	3	4	5	6	7	10	10	10	11	12	13	14	15	16	17	18	19	20	-	0.94	0.22	1.09	2.30	↑72	↑45	↑100	↑100
	σ	1	1	1	1	1	1	1	1	1	1	1	1	1	1	1	1	1	1	-								
7. Variable widths	μ	3	4	5	6	7	8	9	10	11	12	13	14	15	16	17	18	19	20	-	0.80	0.11	0.00	3.20	↑46	↑18	0.0	↑69
	σ	1	1.3	3.2	0.9	1.8	1.7	2.8	0.4	2.7	1.9	0.5	1.9	1.7	1.8	2.3	1.9	2.5	1	-								
8. Variable widths & means	μ	3.5	3.8	6.2	7.7	7.8	9.2	10	11	11	12	12	13	14	15	15.3	16.4	18.5	20	-	0.88	0.27	4.54	4.80	↑44	↑19	↑22	↑50
	σ	1	1.3	3.2	0.9	1.8	1.7	2.8	0.4	2.7	1.9	0.5	1.9	1.7	1.8	2.3	1.9	2.5	1	-								
9. Bimodal in E8+6	μ	3	4	5	6	7	8	9	10	11	12	13	14	15	16	17	18	19	20	14	1.36	0.22	1.00	5.40	↑62	↑55	↑100	↑70
	σ	.5	.5	.5	.5	.5	.5	.5	.5	.5	.5	.5	.5	.5	.5	.5	.5	.5	.5	.5								
10. Bimodal in E8+10	μ	3	4	5	6	7	8	9	10	11	12	13	14	15	16	17	18	19	20	18	1.33	0.22	1.00	5.20	↑73	↑64	↑100	↑73
	σ	.5	.5	.5	.5	.5	.5	.5	.5	.5	.5	.5	.5	.5	.5	.5	.5	.5	.5	.5								
		(*i*)																		(*ii*)	(*iii*)				(*iv*)			

Column (ii) contains the electrode location of the second mean (E_{bim}) for the bimodal conditions 9 and 10.
The results were obtained averaging across 20 individual runs and six SNR values [dB]: 0, 5, 10, 15, 20 and $+\infty$. Values for STAGE II are reported as percent improvement on error values from STAGE I.

This article has been accepted for publication in a future issue of this journal, but has not been fully edited. Content may change prior to final publication. Citation information: DOI 10.1109/TBME.2015.2476373, IEEE Transactions on Biomedical Engineering

amount, and are labelled Υ_μ and Υ_σ, respectively; the "fixed amount" is 1 electrode for the computation of Υ_μ, and 50% from the original value for the computation of Υ_σ. The results for the four metrics over the ten conditions are reported as function of SNR in Fig. 3. Average results for a subset of SNR are reported in columns (*iii*) and (*iv*) of TABLE 1. Conditions 8, 9 and 10 yielded larger errors than other conditions for PECAP STAGE I (red curves). This is somewhat expected since the high variability in the expected means (condition 8) and the bimodality (conditions 9 and 10) violate one or more assumptions made by the PECAP method in STAGE I. For instance, the unimodal Gaussian activation patterns assumed in STAGE I will fail to detect the second mean and width for the bimodal pattern in E8 of conditions 9 and 10.

The addition of STAGE II allowed a better modelling for these conditions. Note that, while bimodal fitting in STAGE II increases the degrees of freedom of PECAP, thus potentially allowing only nonnegative improvements of the fitting between observed and reconstructed *measurement matrix* $\boldsymbol{M}$, larger RMSE could in principle have been observed between true and reconstructed *activation pattern* $\boldsymbol{A}$. This was not observed and improvements relative to errors from STAGE I were reported in the range of 0 (no exception detected) and 100%, as shown in columns (*iv*) of TABLE 1. Note that the errors remaining after STAGE II were likely influenced by the fact that our present implementation of STAGE II corrects only for single exceptions.

Overall, error functions for STAGE I and II in Fig. 3 approach zero for SNR values greater than about 5dB.

B. *Test 2: Human data*

1) Data measurement

Five independent ECAP datasets were measured from four users of the CI24RE implant manufactured by Cochlear® (CIC4 chip). Data reported as S4 and S5 are from the same CI user, after first and second implantation, respectively. The forward-masking procedure described earlier was employed [10, 11]. Two consecutive runs were measured placing the recording electrode either two electrodes basally (for subject S1), or two electrodes apically (for S2, S3) relative to the probe; a spacing of one electrode was used when the assigned recording electrode was used as masker. Only one run was available for S4 and S5. Note that the choice of recording electrode has a considerably smaller effect than the masker-probe separation, because the ECAP is conducted along the length of the cochlea [12], and this effect is thus neglected in the model. Eighteen probe electrodes were tested, leading to 324 (m, p) combinations. The total number of recordings was therefore 2592 (2 recording electrodes × 4 measures [*a*, *b*, *c* and *d* in Fig. 1] × 324) repeated 50 times at a rate of 80 Hz, thus leading to a total recording time of 27 minutes. Each electrode was stimulated at MCL, which was estimated by manually increasing current levels and asking the subject to report the perceived loudness on an eleven-point loudness chart, where MCL corresponded to point 7, labelled "*MOST COMFORTABLE. You could listen to this level for a long time without discomfort*". Measured MCLs did not vary significantly within subject: the standard deviation across electrodes was within 6 μA, and the largest difference for any two electrodes was 20 μA. When the masker and probe were on the same electrode they had the same level. All pulses were charge-balanced biphasic pulses 25 μs in duration, and stimulation mode was monopolar. The return ground was MP1 for the stimulating electrode and MP2 for the recording electrode. The ECAP amplitudes were extracted from the average ECAP as the amplitude difference between the first negative and positive peaks (N1 and P1, respectively). An ECAP was considered valid if N1 occurred between 156 μs and 497 μs of the recorded segment, and if P1 occurred at least 48.8 μs after N1 and before 888 μs. Example ECAPs are reported in Fig. 4.

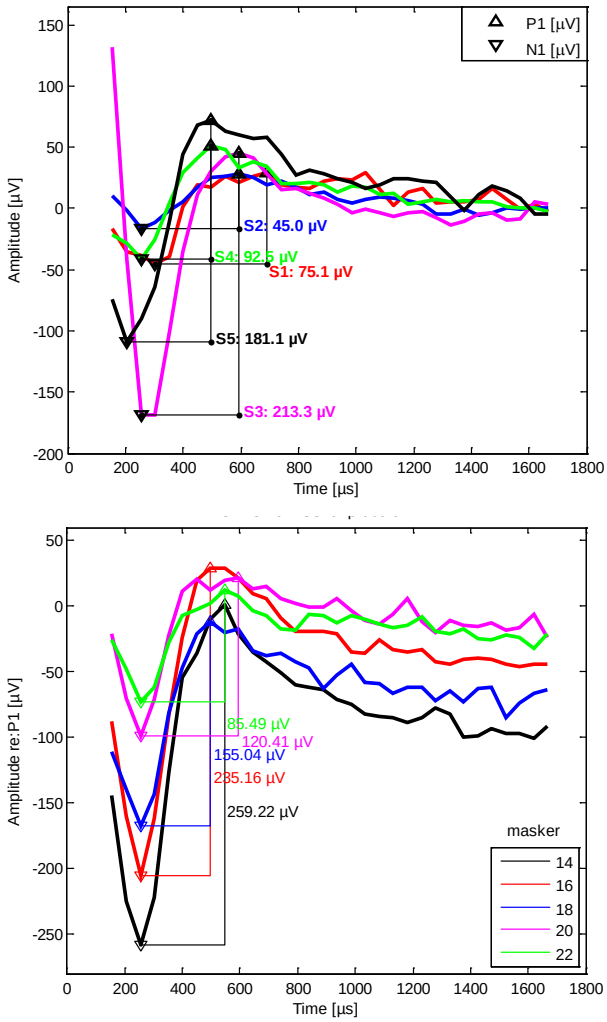

Fig. 4. Typical ECAP responses. Top plot: ECAP responses measured for all subjects when both probe and masker are on electrode 8. ECAP amplitudes (which are used to populate matrix $\boldsymbol{M}$) were computed from N1 and P1 reported as downward and upward facing triangles, respectively. Bottom plot: ECAP measured for S3 as function of masker electrode position. The probe electrode was E14, whereas the masker electrodes were E14, E16, E18, E20 and E22. Color image online.

This article has been accepted for publication in a future issue of this journal, but has not been fully edited. Content may change prior to final publication. Citation information: DOI 10.1109/TBME.2015.2476373, IEEE Transactions on Biomedical Engineering

TABLE 1. ESTIMATED ELECTRODE MEANS (WIDTHS) AFTER STAGE II (SP) AND (BI) USING HUMAN DATA OF TEST 2 AND 3.

	Results from Test 2		*Results from Test 3*		
	STAGE II (SP)	**STAGE II (BI)**	**STAGE II (SP)**	**STAGE II (BI)**	***E in BP***
S1	x	x	x	3(6) - 16.2(6)	3 - 12
S2	12(3.1)→13.5(2.7)	12(1.1) - 15.7(2.3)	-	-	-
S3	x	x	x	8(2) - 18.2(1.5)	8 - 18
S4	x	5(5.8) - 22(6)	-	-	-
S5	x	x	x	11.8(6) - 21.5(1.7)	12 - 22
	(*i*)	(*ii*)	(*iii*)	(*iv*)	(*v*)

Values in parenthesis are estimated widths. The mean (width) values to the left and right of the arrow in column (*i*) indicate the mean (width) values after STAGE I and after STAGE II (SP), respectively. Values in column (*ii*) and (*iv*) are the estimated bimodal parameters after STAGE II (BI).

2) Reconstruction of AP via PECAP

The ***M***s from five ECAP datasets were analysed with the PECAP method and results summarizing detection of exceptions in the excitation pattern are reported in TABLE 2. Note that, although we do not know the true value of ***A*** for the human data, the fitting algorithm minimises the fit between the observed and reconstructed ***M***, which is available. Possible exceptions were found for S2 and S4.

For S2, STAGE II detected one instance of a shifted peak and one of bimodality, both on electrode 12. Allowing a bimodal activation pattern on E12, with second peak 3.7 electrodes more apically, improved the fitting by 12.6%, whereas the shifted peak showed an improvement of 10.6%, hence just above the significant level β set to 10% (see Eq. 11). A shifted peak in the excitation pattern is often interpreted as an instance of a dead region, whereas bimodal APs have been linked with cross-turn stimulation [13-15]. Modelled ***A*** and ***M*** following STAGE I and II are shown in Fig. 5. Overall, results are consistent with an exception around E12; it is possible that a region of lower neural density is found near E12, and that stimulating E12 produces another focus of excitation more basally.

An instance of bimodality was detected also for S4, where modelling the activation pattern on E5 as a bimodal Gaussian with second peak on E22, led to a reduction in the error (see Eq. 9 and Eq.11) of 15.3%. Interestingly, the data after re-implantation of the same subject (reported as S5 in this study) do not show any bimodality. Re-implantation for S4 was motivated by poor subject performance, possibly due to a faulty first device.

C. Test 3: Simulated bimodality in human data

1) Data measurement

In order to further assess the PECAP ability to detect instances of bimodality from ECAP measurements, bimodality was artificially introduced in the data by means of bipolar stimulation. One channel in the array was stimulated in bipolar mode with electrode separation of +9 or +10 between the two stimulated electrodes in each bipolar pair, in order to mimic cross-turn stimulation [15]. The channel in bipolar mode was E3 for S1, E8 for S3 and E12 for S5 (see column (*v*) in TABLE 2). Data from S2 and S4 were excluded as instances of bimodality had already been shown in Test 2. The data collection procedure described in III.B.1 was adopted also for Test 3.

2) Results

Results are reported in column (*iii*) and (*iv*) of TABLE 2. Instances of bimodality were detected in all three subjects after STAGE II of PECAP. The activation pattern for the electrode stimulated in bipolar mode was always better modelled by PECAP using a bimodal Gaussian function, which overall reduced the error between the measured and modelled ECAP measurement ***M*** by more than 10%. No shifted peak was detected, consistent with results from Test 2.

D. Operating SNR for PECAP based on human data

1) Test-retest reliability

The PECAP approach is intended as a first step towards the development of an objective diagnostic tool to detect exceptions in electrode-to-neuron mapping of cochlear implant users. The output of such a tool may inform different stimulation strategies that can affect the outcome of the device for individual subjects. As such, it is crucial to determine the lowest SNR at which the PECAP can be reliably applied. From the computer simulation in Test 1, acceptable errors were obtained for SNR of 5 dB or higher (Section III.A.2; Fig. 3). This was determined by tracking four performance measures as a function of SNR and using ten artificial conditions (see TABLE 1). Note that this value is dependent on the exact conditions that have been simulated.

Having determined the operating SNR for ECAP, it is necessary to estimate the amount of SNR that is found in physiological data. We determined this value using ECAP data of Test 2. The RMSE between the ***M*** of two simulated runs was compared against the RMSE between two consecutive measurements of ***M***, which were available for S1, S2 and S3. Both simulated and actual ***M***s were linearly normalised before RMSE computation.

2) Results

Fig. 6 reports the RMSE obtained for simulated and for

This article has been accepted for publication in a future issue of this journal, but has not been fully edited. Content may change prior to final publication. Citation information: DOI 10.1109/TBME.2015.2476373, IEEE Transactions on Biomedical Engineering

physiological $\boldsymbol{M}$s. The RMSE for simulated $\boldsymbol{M}$s as function of input SNR was fitted with a 5th order polynomial. The intercept of the fit with the RMSE measured from physiological data is indicative of realistic SNRs in human data. A SNR greater than 5 dB was found for the three subjects, therefore within the PECAP operating SNR range. In general, for subjective data where the RMSE between two ECAP runs corresponds to SNR smaller than 5 dB, the PECAP reconstruction may not be reliable. A reliable behaviour of the approach was defined as low misestimation of means (Υ_μ) and widths (Υ_σ) of the Gaussian APs and the ability of detecting single instances of bimodality or displaced means.

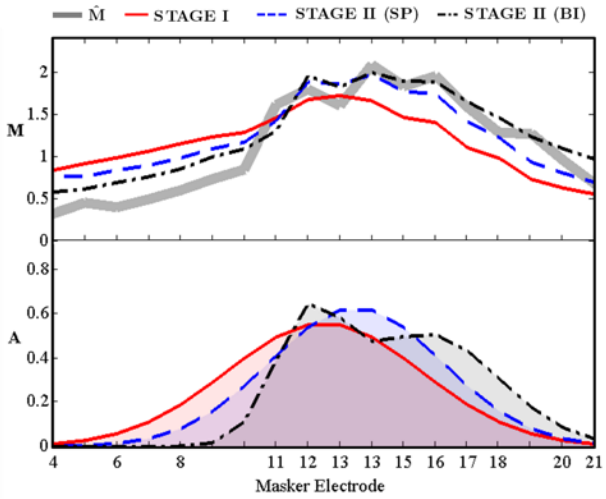

Fig. 5. Top panel: measured and modelled $\boldsymbol{M}$ for S2 on E12; bottom: modelled $\boldsymbol{A}$ after STAGE I, STAGE II to detect shifted peaks (SP), or STAGE II to detect bimodality (BI). Color image online.

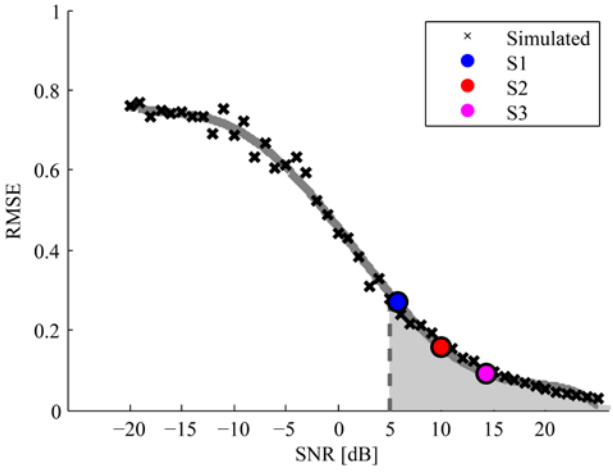

Fig. 6. Test re-test variability. RMSEs obtained from two runs of simulated $\boldsymbol{M}$'s at various SNR (×). RMSEs obtained from human data are also plotted (o) on the intercept with the polynomial fit. The shaded area indicates the SNR space in physiological measurements where PECAP outcomes are reliable. Color image online.

IV. Discussion

The present study describes a novel approach to recover neural activation patterns from ECAP amplitudes. The approach, termed PECAP, consists of two stages that combine a highly constrained and a less-constrained optimization to ensure convergence. Constraining is necessary because the solution is generally not unique. The PECAP was shown to be able to predict both simulated and measured data for realistic SNR values. The multi-stage approach includes a search for two types of exceptions in the excitation pattern: shifted peaks or bimodality. A number of limitations of the PECAP and further discussion points are reported below.

A. *On the symmetry assumption*

ECAP amplitudes reflect the joint neural activation pattern of both masker and probe activation patterns; as such, any two electrodes should produce the same ECAP amplitude irrespective of which is used as masker and which as probe. While the theoretical bases for this mechanism have been described in other studies, it has often been neglected from the interpretation of the data, with ECAPs being used as a direct measure of the probe's excitation [4, 16, 17]. In the present study, a symmetry assumption was incorporated in the ECAP model (Eq. 2-3), which is used by the proposed PECAP algorithm to recover activation patterns.

B. *On the shape of the activation patterns*

In II.A it is assumed that AP patterns can be described by Gaussian functions each with a single mean. While the unimodality assumption is relaxed through STAGE II, this remains possible for only one channel at the time. In normal, acoustic hearing the excitation patterns of the masker and probe have flat tops and steep low-frequency skirts [18]. The exact shape of the excitation patterns in CI cannot be generalised for all CI users, however, based on forward and interleaved masking experiments, it is likely to be some variation of a bell-shaped pattern [19-21].

A related assumption is made on the area of the activation patterns (see II.A.*iii*). Specifically, it is assumed that the area under the excitation pattern for a given stimulus should reflect the perceived loudness of such stimulus. There is some evidence that this is the case for acoustic hearing [22].

C. *Robustness of the algorithm*

The current implementation of the PECAP algorithm suffers from two limitations. First, STAGE II of the PECAP algorithm is limited to the detection of a single exception. When multiple instances of shifted peaks and/or bimodality (e.g., dead regions and cross-turn stimulation) occur in the same subject, the AP reconstructed using PECAP is likely to be inaccurate.

Second, the algorithm is dependent on the arbitrary choice of certain parameters, such as β, the constraints in Eq. 10, or the optimization algorithm.

Further investigation of these aspects is essential, as the robustness of the algorithm has particular relevance when considering its clinical applicability as diagnostic tool.

D. Operating SNR for PECAP

ECAP measurements reflect a combination of neural activity and measurement noise. Depending on factors such as the equipment used for data collection, the procedure in place or the subject, the SNR in the measured ECAPs may vary considerably. The PECAP approach would provide different degrees of accuracy depending on the SNR in the human data. Being able to determine what is the lowest SNR in the human data at which the PECAP can provide a reliable solution has obvious clinical relevance. In section III.D, this value was determined to be 5 dB, which was smaller than the corresponding SNRs found in human data of this study. It is important to note, however, that for activation patterns that are different from those simulated in III.A a different operating SNR may be necessary for reliable predictions of PECAP.

CONCLUSION

A novel algorithm – termed PECAP – was described that can recover neural activation patterns from evoked compound actions potentials in cochlear implant users. The algorithm performs multi-stage optimizations to model gaussian activation patterns and to detect single exceptions in the expected patterns, such as bimodality or shifted peaks. PECAP performed reliably on both computer simulated and actual human data from this study. The algorithm has potential as clinical tool for CI users.

ACKNOWLEDGMENT

The authors would like to thank Steven M. Bierer and Julie A. Bierer for their insights during earlier stages of this work, and two expert reviewers for their helpful comments.

REFERENCES

[1] C. McKay, *et al.*, "Can ECAP Measures Be Used for Totally Objective Programming of Cochlear Implants?," *Journal of the Association for Research in Otolaryngology*, vol. 14, pp. 879-890, 2013/12/01 2013.

[2] H. Thai-Van, *et al.*, "Modeling the relationship between psychophysical perception and electrically evoked compound action potential threshold in young cochlear implant recipients: clinical implications for implant fitting," *Clinical Neurophysiology*, vol. 115, pp. 2811-2824, 2004.

[3] S. Vlahović, *et al.*, "Differences between electrically evoked compound action potential (ECAP) and behavioral measures in children with cochlear implants operated in the school age vs. operated in the first years of life," *International Journal of Pediatric Otorhinolaryngology*, vol. 76, pp. 731-739, 2012.

[4] L. T. Cohen, *et al.*, "Spatial spread of neural excitation in cochlear implant recipients: comparison of improved ECAP method and psychophysical forward masking," *Hearing Research*, vol. 179, pp. 72-87, 2003.

[5] C. J. Brown, *et al.*, "Electrically evoked whole-nerve action potentials: Data from human cochlear implant users," *The Journal of the Acoustical Society of America*, vol. 88, pp. 1385-1391, 1990.

[6] M. L. Hughes and L. J. Stille, "Effect of Stimulus and Recording Parameters on Spatial Spread of Excitation and Masking Patterns Obtained With the Electrically Evoked Compound Action Potential in Cochlear Implants," *Ear & Hearing*, vol. 31, pp. 679-692, 2010.

[7] C. C. Finley, *et al.*, "Role of Electrode Placement as a Contributor to Variability in Cochlear Implant Outcomes," *Otology & Neurotology*, vol. 29, pp. 920-928, 2008.

[8] J. A. Undurraga, *et al.*, "Evaluating the Noise in Electrically Evoked Compound Action Potential Measurements in Cochlear Implants," *Biomedical Engineering, IEEE Transactions on*, vol. 59, pp. 1912-1923, 2012.

[9] R. H. Byrd, *et al.*, "A trust region method based on interior point techniques for nonlinear programming," *Mathematical Programming*, vol. 89, pp. 149-185, 2000/11/01 2000.

[10] P. J. Abbas, *et al.*, "Channel Interaction in Cochlear Implant Users Evaluated Using the Electrically Evoked Compound Action Potential," *Audiology and Neurotology*, vol. 9, pp. 203-213, 2004.

[11] C. Miller, *et al.*, "Electrical Excitation of the Acoustically Sensitive Auditory Nerve: Single-Fiber Responses to Electric Pulse Trains," *JARO - Journal of the Association for Research in Otolaryngology*, vol. 7, pp. 195-210, 2006.

[12] M. L. Hughes and L. J. Stille, "Effect of stimulus and recording parameters on spatial spread of excitation and masking patterns obtained with the electrically evoked compound action potential in cochlear implants," *Ear and Hearing*, vol. 31, pp. 679-692, 2010.

[13] J. H. Goldwyn, *et al.*, "Modeling the electrode–neuron interface of cochlear implants: Effects of neural survival, electrode placement, and the partial tripolar configuration," *Hearing Research*, vol. 268, pp. 93-104, 2010.

[14] B. C. J. Moore and J. I. Alcantara, "The Use of Psychophysical Tuning Curves to Explore Dead Regions in the Cochlea," *Ear & Hearing*, vol. 22, pp. 268-278, 2001.

[15] J. H. M. Frijns, *et al.*, "The Importance of Human Cochlear Anatomy for the Results of Modiolus-Hugging Multichannel Cochlear Implants," *Otology & Neurotology*, vol. 22, pp. 340-349, 2001.

[16] M. L. Hughes and L. J. Stille, "Psychophysical versus physiological spatial forward masking and the relation to speech perception in cochlear implants," *Ear and Hearing*, vol. 29, p. 435, 2008.

[17] M. L. Hughes and L. J. Stille, "Psychophysical and physiological measures of electrical-field interaction in cochlear implants," *The Journal of the Acoustical Society of America*, vol. 125, pp. 247-260, 2009.

[18] B. C. J. Moore and B. R. Glasberg, "Suggested formulae for calculating auditory-filter bandwidths and excitation patterns," *The Journal of the Acoustical Society of America*, vol. 74, pp. 750-753, 1983.

[19] J. A. Bierer, *et al.*, "Identifying Cochlear Implant Channels With Poor Electrode-Neuron Interfaces: Electrically Evoked Auditory Brain Stem Responses Measured With the Partial Tripolar Configuration," *Ear & Hearing July/August*, vol. 32, pp. 436-444, 2011.

[20] D. A. Nelson, *et al.*, "Forward-masked spatial tuning curves in cochlear implant users," *The Journal of the Acoustical Society of America*, vol. 123, pp. 1522-1543, 2008.

[21] M. Azadpour, *et al.*, "Place specificity measured in forward and interleaved masking in cochlear implants," *The Journal of the Acoustical Society of America*, vol. 134, pp. EL314-EL320, 2013.

[22] Z. Chen, *et al.*, "A new method of calculating auditory excitation patterns and loudness for steady sounds," *Hearing Research*, vol. 282, pp. 204-215, 2011.